Ramifications of Isotropic Sampling and Acquisition Orientation on DTI Analyses

D. H. Laidlaw[1], S. Zhang[1], M. E. Bastin[2,3], S. Correia[4], S. Salloway[4,5], P. Malloy[4]

[1]Computer Science, Brown University, Providence, RI, United States, [2]Medical and Radiological Sciences, University of Edinburgh, Edinburgh, United Kingdom, [3]West General Hospital, Edinburgh, United Kingdom, [4]Dept. of Psych. and Human Behavior, Brown Medical School, Providence, RI, United States, [5]Department of Clinical Neurosciences, Brown Medical School, Providence, RI, United States

Introduction - Six diffusion tensor imaging (DTI) datasets of a normal volunteer were acquired and analyzed to investigate differences in analysis results due to acquisition orientation and sampling anisotropy.

Methods - The head of a normal volunteer was imaged in a Siemens Symphony 1.5T scanner. Three slice packets were acquired axially. Slices were 5mm thick with 0.1mm spacing. The second slice packet was translated in the slice direction 1.7mm and the third 3.4mm. Each slice was acquired with a 128x128 matrix and interpolated to 256x256. The field of view was 217mm; in-plane sample spacing was 0.85mm. Siemens' MDDW protocol was used, with three *b* values (0, 500, 1000) in 12 directions. A fourth axial dataset was synthesized from the first three by interleaving all of the slices and zero-filling in the slice direction; the resulting inter-slice distance was 0.85mm. Note that the fourth dataset is sampled isotropically and has six times the samples of each of the initial three datasets -- zero-filling doubles the number of slices. Three sagittal datasets were acquired analogously and a fourth isotropic sagittal dataset synthesized from the three. The inferior boundary of the sagittal and axial scans was matched. Diffusion tensors were fit to each of the datasets using a non-linear fitting method [1].

For scalar analysis, the diffusion rate at each sample point was characterized as linear, planar, or spherical (isotropic) in accordance with Westin's diffusion metrics, *l*, *p*, and *s* [3]. Sample points where $s > 0.77$ were labeled isotropic; remaining samples were labeled either linear if $l > p$ or planar if not. Next, the midline of the brain was identified in coronal slices within each of the axial and sagittal datasets. A region of interest (ROI) containing the corpus callosum and measuring 40x40x20 mm, with the short direction axial, was then defined across the midline. The percentage of spherical, linear, and planar sample points within each half of the ROI was measured [2].

For each dataset, streamtubes and streamsurfaces were calculated over the same ROI to show linear and planar diffusion, respectively [4]. Tensor analysis was performed visually using an interactive 3D display device.

Results and Discussion - Table 1 shows the percentage of each type of diffusion in the right and left halves of the region of interest. Note that the differences between the axial and sagittal acquisitions are generally less than the differences between isotropic and anisotropic sampling, although all differences are relatively small. This is consistent with an interpretation that isotropic sampling in either direction produces the same results and that the additional samples in the more finely sampled isotropic cases reduce the effects of noise by averaging. It is interesting to note that in a corresponding analysis of the whole head, the differences were greater between the axial and sagittal acquisitions than between the isotropic and anisotropic sampling. The different pattern of results may reflect imaging artifacts that change the diffusion classification near boundaries of materials with different magnetic susceptibilities. Such boundaries were not present in the ROI we analyzed.

Figure 1 shows visual representations of the four combinations of axial vs. sagittal and isotropic sampling vs. anisotropic sampling. In both cases of isotropic sampling the visual results are qualitatively the same -- they show the same major white matter structures. The two cases with anisotropic sampling differ both from the isotropic sampling cases and from one another, demonstrating a bias due to imaging direction. In the sagittal acquisition with anisotropic sampling the cingulum bundle and some parts of the internal capsule are missing from the visualization. In the axial acquisition with anisotropic sampling the corpus callosum is broken.

Conclusions - The relatively small differences in the scalar analysis suggest that for scalar statistical analyses of structures larger than the imaging resolution and in regions well away from susceptibility boundaries, isotropic sampling may not be needed, and imaging direction does not appear to have a significant impact on values. However, for analyses incorporating connectivity information, anisotropic sampling can lead to orientation-related bias and isotropic sampling may be indicated.

References - [1] Ahrens et al. 1998 Magn. Reson. Med. 40, 119-132; [2] Zhang et al. 2003 Magn. Reson. Med, in press; [3] Westin et al. 1997, Proc. ISMRM; [4] Zhang et al. 2003 IEEE Trans. Visual. Comp. Graph., 9, 454-462.

Figure 1 Streamtubes (red) and streamsurfaces (green) showing linear and planar diffusion, respectively, in an ROI around the corpus callosum. The views are the same in all cases and are from anterior to posterior over the top of the corpus callosum, which runs from left to right across the top have of each image. Isotropic sampling cases are qualitatively similar. Anisotropic cases are missing different white-matter structures.

Table 1 Percentages of samples characterized by linear, planar, and spherical (isotropic) diffusion in ROI by acquisition direction and left vs. right. *l*=linear diffusion, *p*=planar diffusion, *s*=spherical (isotropic) diffusion.

	Isotropic Sampling	Anisotropic Sampling
Sagittal Acquisition		
Axial Acquisition		
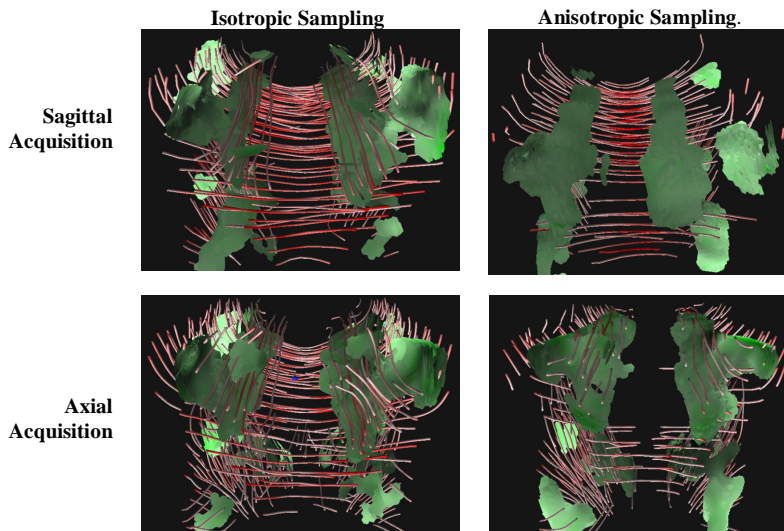
Sampling	Sagittal/Left *l*	*p*	*s*	Sagittal/Right *l*	*p*	*s*
Isotropic	32.7	22.6	44.7	35.1	22.5	42.4
Aniso. 1	34.3	26.9	38.7	32.4	19.7	48.0
Aniso. 2	30.1	23.5	46.4	34.7	21.8	43.5
Aniso. 3	30.7	18.2	48.1	38.8	24.2	37.0

	Axial/Left *l*	*p*	*s*	Axial/Right *l*	*p*	*s*
Isotropic	33.4	20.5	46.1	35.9	20.9	43.2
Aniso. 1	34.5	21.4	44.0	35.0	23.3	41.7
Aniso. 2	35.3	22.0	42.7	37.0	21.5	41.5
Aniso. 3	30.7	18.8	50.5	35.2	18.8	46.0